1

Challenges in Microflow Measurements

Boguslaw Kruczek and Siamak Lashkari
University of Ottawa
Department of Chemical & Biological Engineering
Canada

1. Introduction

The term "microflows" is often associated with microfluidics, which is a multidisciplinary field intersecting engineering, physics, chemistry, microtechnology, and biotechnology that has emerged in the beginning of the 1980s. Improvements in fabrication of microflow devices such as micropumps, microvalves, microheat exchangers, and other microcomponents and sensors have led to the rapid development of microfluidics in the last decade (Morini, 2011). For this reason, many studies have been conducted to verify if the laws governing transport phenomena within channels of macroscopic dimensions are applicable at the microscale. These studies clearly show the necessity of correcting the classical theory when applying it to flow in microchannels, but appropriate corrections of the classical theory require reliable measurement of microflows. On the other hand, microflows also originate from a diffusive transport of fluids, typically gases, through seemingly non-porous media, such as perm-selective membranes, packaging materials, and walls of nuclear and chemical vessels. Characterization of materials for gas separation membranes, packages in food industry, walls of chemical and nuclear reactors, which involve determination of diffusivity, permeability and solubility coefficients of different gases in these materials, relies on accurate measurement of microflows.

Microflows, similarly to regular flows, result from a pressure gradient across a medium (e.g. a barrier material or microchannel), and are normally measured downstream from the medium. While the term microflow may refer to both a liquid and a gas, in this Chapter it will exclusively refer to "very low" flow rates of gases. There is no specific upper limit for microflows, and often flows much greater than 1 cm^3(STP)/min are still considered as microflows in microfluidics literature (Morini et al., 2011). However, in this Chapter we will focus on the flows that are less than 0.1 cm^3(STP)/min, which coincides with the minimum gas flow rate that can be measured directly using commercial volumetric or mass flow meters. Flows in this range are measured indirectly by checking the value taken by other measurable quantities, typically pressure or volume.

Defining gas flow as the number of moles (n) of a particular gas species passing through a system at a given time, the primary measurement is based on an equation of state. For the level of accuracy of flow measurements the ideal gas law suffice:

$$pV = nRT \tag{1}$$

where, p is the absolute pressure, V is the volume of the system, R is the universal gas constant, and T is the temperature. A primary measurement can then be made and the flow rate is given by:

$$Q = \frac{dn}{dt} = \frac{p}{RT}\frac{dV}{dt} + \frac{V}{RT}\frac{dp}{dt} - \frac{pV}{RT^2}\frac{dT}{dt} \quad (2)$$

If two of the three variables (V, p, T) are kept constant while the third one is monitored during the experiment, the flow rate of the gas can be determined. Eq. (2) provides the basis of two techniques for the determination of microflows, namely constant pressure (CP) and constant volume (CV) techniques. In the CP technique the flow is measured by monitoring the change in volume, resulting from the flow, at the conditions of constant temperature and pressure. In the CV technique, on the other hand the flowing gas is accumulated in a tank of known volume and the flow rate is determined from the isothermal rate of pressure increase.

Due to different conditions at which microchannels and semipermeable membranes are operated, the way the CP and CV techniques are used in these applications is different. The challenges in accurate measurements of microflows in microchannels, which mainly arise from the difficulty of keeping two of the three variables strictly unchanged, have been discussed recently by Morini et al. (2011). In case of characterization of semipermeable membranes by the CP and CV techniques, it is easier to keep two of the three variables unchanged. Yet, significant differences in the properties of membranes from the same material are often reported. The objective of this Chapter is to systematically review the challenges in the measurement of microflows; in particular those related to characterization of gas separation membranes.

To accomplish this objective, we will first discuss the importance of accurate measurements of microflows in applications involving characterization of microchannels and membranes, along with the specific information being sought in these characterizations. After these introductory remarks, the discussion will be directed into two parallel streams. The first one is dedicated to the CP technique, with special emphasis on recently developed fully automated soap flowmeter and the phenomenon of back permeation of air in CP systems open to atmosphere. The second one is dedicated to the CV method with special emphasis on the phenomenon of resistance to gas accumulation in high vacuum systems and a step by step procedure for the design of new CV systems.

2. Importance of microflows

Accurate measurement of microflows is indispensable for the characterization of gas separation membranes, packages in food industry, walls of chemical and nuclear reactors, (all of which fall into a category of nonporous materials), as well as, in studies of transport phenomena in microchannels.

2.1 Characterization of nonporous materials

Gas transport in nonporous membranes is commonly described by a solution-diffusion model. In this model, the permeability coefficient (P_m) is a fundamental property of

materials, which is expressed as a product of a thermodynamic factor (S_m) called the solubility coefficient, and a kinetic parameter (D_m) called the diffusion coefficient (Zolondz and Fleming, 1992):

$$P_m = D_m S_m \tag{5}$$

In the solution-diffusion model, the transport of gas i consists of three independent steps. First, a gas is dissolved in a film at a high pressure (feed) side, then the gas diffuses across the film according to Fick's law of diffusion, and finally the gas evaporates from the film at a low pressure (permeate) side. Assuming the applicability of Henry's law, which is a reasonable approximation in the case of dilute solutions, the three steps of the solution-diffusion model are described by the following equations:

Step 1: $$C_{i,f} = S_{m,i}\, p_{i,f} \tag{6}$$

Step 2: $$J_i = -D_{m,i} \frac{dC_i}{dx} \tag{7}$$

Step 3: $$C_{i,p} = S_{m,i}\, p_{i,p} \tag{8}$$

where: C_i is the concentration of component i inside the membrane, p_i is the partial pressure of i in the gas phase, J_i is the diffusive flux, and x is the distance from the feed surface of the membrane. The subscripts f and p refer to the feed and permeate side, respectively.

Assuming that Step 2 is a rate controlling step, and $D_{m,i}$ and $S_{m,i}$ are pressure independent, the solution-diffusion model simplifies to:

$$N_i = \frac{Q_i}{A_m} = \frac{P_{m,i}}{L_m}\left(p_{i,f} - p_{i,p}\right) \tag{9}$$

where: L_m and A_m are the respective film thickness and area, and N_i and Q_i are the respective steady state permeate flux and permeation rate, of gas i in the membrane. It is important to note that because the film is a stationary medium, $J_i = N_i$. Eq. (8) may also be rearranged to:

$$P_{m,i} = \frac{Q_i L_m}{A_m\left(p_{i,f} - p_{i,p}\right)} \tag{10}$$

The selective properties of a film (membrane) for the separation of gases i and j are assessed based on the ratio of permeability coefficients, which is often referred to as permselectivity:

$$\alpha_{ij} = \frac{P_i}{P_j} \tag{11}$$

Gas permeation tests can be carried out with pure gases or gas mixtures. In the former case the partial pressure gradient in Eqs. (9) and (10) becomes the total pressure gradient, and the ratio of permeability coefficients determined with the respective pure gases is referred to as the ideal selectivity. In the latter case, apart from the measurement of the permeation rate, the composition of the permeating gas must also be determined.

The permeability and ideal selectivity of films are determined in steady state permeation experiments using both the CP and CV techniques. On the other hand, the diffusivity is determined in transient gas permeation experiments (time lag method), which are normally carried out using the CV systems.

2.2 Transport phenomena in microchannels

Similarly to the flow in regular conduits, the major objective of transport phenomena in microchannels is to predict the pressure drop at a known average velocity of a fluid, normally a gas, in a microchannel of a specific geometry at known temperature and pressure conditions. However, unlike the regular conduits, rather than setting the flow rate and measuring the resulting pressure drop, the flow rate is measured at a specific pressure gradient across the microchannel. This is due to the current state of technology being unable to produce mass flow controllers capable of controlling flows that are of interest to microfluidics.

While the transport phenomena in regular conduits are adequately described with Navier-Stokes equations, these equations often fail in the case of flows in microchannels, because of rarefactions effects. The range of applicability of Navier-Stokes equations is provided in terms of Knudsen number (*Kn*):

$$\mathrm{Kn} = \frac{\lambda}{\mathrm{D_h}} = \frac{\mu}{\mathrm{D_h p}}\sqrt{\frac{\pi \mathrm{RT}}{2}} \tag{12}$$

where, λ is the gas mean free path, D_h is the characteristic dimension of the channel, μ is the dynamic viscosity of the gas, p and T are the gas pressure and temperature, and R is the gas constant. The departure from Navier-Stokes equations starts at $Kn > 0.001$. The flows with $0.001 < Kn < 0.3$ are often referred to as slip flows, while those with $0.3 < Kn < 10$ as transition flows. When *Kn* is greater than 10, i.e., when the collisions between gas molecules and microchannel walls are much more frequent than those between gas molecules, the transport occurs in a free molecular regime sometimes referred to as a Knudsen regime. Over the years a number of transport models have been developed to take into considerations the rarefaction effects in the slip and transition flow regimes. Some of these models include: the first order model (Maxwell, 1879), the second-order model (Deissler, 1964), the second-order model with Deissler boundary conditions modified with Hadjiconstantinou's coefficients (Hadjiconstantinou, 2003) that was recently proposed by Pitakarnnop et al. (2010).

The key aspect in verification and development of existing and new theoretical models, as well as semi-empirical ones is the capability of accurate measurement of microflows. The microflows in microfluidics are measured using both the CP and CV techniques.

3. Microflow measurement

Indirect measurements of microflows may involve monitoring of such measurable quantities as pressure, forces, weight, volume, temperature or any combination thereof (Morini et al., 2011). However, in this Chapter we will focus only on two of these quantities, namely volume and pressure, which provide a basis for the constant pressure and constant volume techniques.

3.1 Constant pressure technique

In the constant pressure (CP) technique, the flow measurements are carried out at constant pressure and temperature conditions, while changes in volume are monitored simultaneously. Consequently, Eq. (2) simplifies to:

$$Q = \frac{dn}{dt} = \frac{p}{RT}\frac{dV}{dt} \tag{13}$$

The simplest and oldest example of a CP instrument is a soap flowmeter, which is commonly used for quick determination of gas permeability in membranes. Soap flowmeters are also used for measurements of microflows emerging from microchannels (Celata et al., 2007). However, the latter application more frequently utilizes a liquid droplet tracking (DT) method, which similarly to a soap flowmeter utilizes a calibrated tube for the actual measurements. While a soap flowmeter is operated in a vertical position, the tube in the DT method is normally operated horizontally. The velocity of the gas is determined in both cases by recording the position of a soap bubble/liquid droplet versus time. Furthermore the flow rate of the gas can be calculated, knowing the diameter of the calibrated tube (d_t). In this case Eq. (13) can be re-written as:

$$Q = \frac{p}{RT}\frac{\pi d_t^2}{4}\frac{\Delta l}{\Delta t} \tag{14}$$

It is important to note that the term "constant pressure" is also used in reference to complex instruments, which utilize a piston or a bellow controlled by an automation system to allow volume variation while maintaining a constant pressure. Examples of these instruments, which are technologically difficult to implement, are provided by McCulloh et al. (1987) and Jousten et al. (2002). These instruments are not however, discussed in this Chapter.

The main advantage of the CP technique is that it operates based on measurements of primary units, the time and volume (length). As a result, there is no correlation which could change over time and thus, there is no need to recalibrate instrument over time.

3.1.1 Soap flowmeter

The scientific description of soap flow meters was first revealed by Exner (1875), and since then these instruments have been widely used in different applications involving manual gas flow measurements. A schematic diagram of a typical soap flowmeter, outlining four key sections of the instrument, is shown in Fig. 1. The bottom part accommodates a rubber bulb containing soap, a side aperture for the gas influx, and a smooth intersection to hold a small residual of soap from which the bubble is formed. The purpose of this part is to create a bubble and to transfer it to the main tube. The second part is a part of the tube above the side aperture for the gas influx where the created bubble accelerates and reaches a constant velocity. The length of this part depends on the gas flow rate as well as on the diameter of the tube. In most flowmeters this part is very short compared to the length of the main tube. The third part is a graduated tube where the actual measurement takes place. The bubble moving in the calibrated tube should have a constant velocity, which requires a constant pressure difference across the bubble. A smooth glass wall, which is well lubricated with a

soap falling down, provides a frictionless path for the soap bubble to rise. The last part is the end section of the tube, in which the bubbles break up thus creating the falling liquid soap which lubricates the tube walls. The end section should not be used for the measurement purposes because back diffusion of air may significantly affect the velocity of the bubble in this part (Czubryt and Gesser, 1968; Guo and Heslop, 2004).

In order to produce a bubble in a typical soap flowmeter shown in Fig. 1, the rubber bulb must be squeezed to push the liquid soap into the tube. When the liquid level is above the inlet gas tube, the liquid is held for a short time to wet the glass, after which the rubber bulb is released leaving, some residual liquid at the intersection with the gas inlet; this residual liquid is pushed inside the main tube, forming a bubble. The produced bubble must be thin, yet strong enough to pass through the calibrated part of the tube without breaking up. There are several parameters affecting the properties of the bubble. One of the parameters is the properties of the soap solution. The common solution is a mixture of glycerol, distilled water, and a surfactant. The influence of soap properties on the flow measurement are discussed in the literature (Barigou and Davidson, 1994).

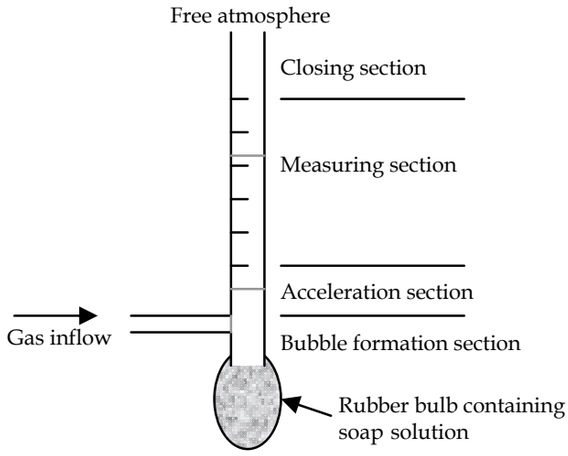

Fig. 1. Schematic diagram of typical soap flowmeter (Lashkari and Kruczek, 2008A).

It is generally believed that in order to make a thin bubble the time interval for holding the liquid in the tube should be very short, and by increasing the holding time, the curvature of the produced bubble will increase. In turn, the greater the curvature of the bubble the more liquid will be carried out by the bubble. Experimental data and equations relating the amount of liquid with the diameter of the bubble in vertical tubes are presented and discussed in the literature (Barigou and Davidson, 1994). On the other hand, Heslop et al. (1995) showed that there is a range of the liquid amount from which meta-stable bubbles can be formed.

The resolution of a soap flowmeter and hence the minimum gas flow rate that can be measured using this instrument depends on the size of the calibrated tube. To our best knowledge, the smallest commercial soap flowmeter (available from SEG) has the nominal size of 50 μL and allows the measurements of gas flow rates as low 0.005 mL/min. In principle, one could increase the resolution of a soap flowmeter by decreasing the diameter of the tube, which was actually suggested by Levy (1964) and Arenas et al. (1995). However,

there is a critical radius of the tube (r_{cr}), below which a bubble cannot be formed, and instead of a bubble a liquid column (droplet) is formed. For fully wetting liquids in a vertical capillary Concus (1968) calculated the critical Bond number (B_{cr}) below which a bubble cannot be formed:

$$B_{cr} = \frac{\rho g r_{cr}^2}{\sigma} = 0.842 \tag{15}$$

where: ρ and σ are the density and the surface tension of the soap liquid solution, and g is the gravity constant. The concept of B_{cr} also explains why the liquid solution used in bubble flow meter should contain a surfactant. If instead of a bubble a liquid droplet is formed, one can still carry out flow measurements. However, these measurements would fall into the category of DT methods, which will be discussed in the next section.

Flow measurements using soap flowmeters are normally performed manually, i.e. by squeezing a rubber bulb to push the soap liquid above a side aperture, visually observing the movement of a bubble in the calibrated tube and recording the time using a stopwatch. However, since more than a decade ago, there are commercially available soap flowmeters employing optical sensors for automatic detection of the soap bubble passing through the flowmeter, similar to those described by Arenas et al. (1995). The commercially available SF-1/2 and Optiflow supplied by STEC and Supelco tubes, respectively, utilize a timer-trigger mechanism for bubble detection. The flow rates that can be measured with Optiflow Flowmeter start from 0.1 cm^3/min, which is more than one order greater than what can be measured manually. The corresponding accuracy of this instrument is 3% of the reading. In addition to automatic flow measurements, the SF-1/2 soap flowmeter, available from STEC, is a fully automated instrument, with the bubble making mechanism based on the principle discussed by Bailey et al. (1968). Essentially, the bubble is made by pushing the liquid to touch the bottom of the flowmeter tube. This mechanism, however, is suitable for the flow rates (0.2-1000 mL/min) that are greater than those which are of interest in this Chapter.

3.1.2 Novel fully automated soap flowmeter

Recently, the current authors reported the development of novel, fully automated soap flowmeters for microflow measurements. The new instruments are based on existing soap flowmeters, in which the bubble maker and the calibrated tube are modified (Lashkari and Kruczek, 2008A).

Fig. 2 presents a schematic diagram of an automated bubble-making device developed by Lashkari and Kruczek (2008A). In order to make the process fully automated, a computer-controlled three way solenoid valve, a needle valve, a low pressure regulator and a sealed soap container are used. When the three way valve is opened by a computer signal, a low external pressure, less than 1 psig, is applied on the surface of the soap liquid in the sealed container. To avoid a sudden pressurization of the liquid soap, which would cause a jump and splash of the liquid on the tube walls, a needle valve is installed between the low pressure regulator and the three way solenoid valve. This allows pushing slowly the soap liquid inside the flowmeter tube and forming a soap bubble in front of the gas inlet to the main tube. The final height of the liquid in the tube depends on the applied pressure and the ratio of the area of the liquid soap container to the cross sectional area of the tube. Then, the

solenoid valve is closed and the pressure on the liquid soap is released through the vent. This allows removing excess liquid from the tube back to the soap container.

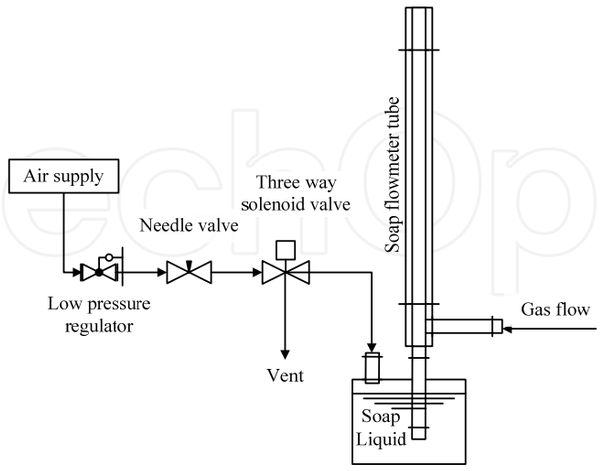

Fig. 2. Schematic diagram of a traditional soap flowmeter with an automated soap bubble maker apparatus. Adapted from Lashkari and Kruczek (2008A)

Usage of a computer controlled instrument makes it possible to adjust the time interval for holding liquid inside the tube. Consequently, the bubbles can be produced in the same way in all the experiments. This is one human error, which can be easily eliminated using the automated bubble maker shown in Fig. 2. The actual holding time of the liquid inside tube depends on its size. For example, for a 500 µL flowmeter, 0.3 second was determined to be a sufficient residence time for the soap liquid in the tube to make a thin, yet strong layer of soap at the gas entrance (Lashkari and Kruczek, 2008A). It is important to note that such a short residence time would not be attainable if the bubble were made manually by squeezing a rubber bulb. Moreover, since opening and closing of the solenoid valve is controlled by a computer program, the measurements of the flow rate can be executed automatically in a pre-scheduled routine.

The other part that was modified in the developed instrument was the calibrated tube. Fig. 3 presents a schematic of light emitting diodes (LEDs) and their corresponding photo diode sensors installed on a 500 µL Supelco soap flowmeter. The distance between any two adjacent sensors is restricted by the size of the photodiodes, and in Fig. 3 this distance is approximately 1/2 inch. The space for the light to pass into the photodiode measures about 1/16 inch. When a bubble passes through the light, the photodiode voltage is reduced due to the curvature of the bubble meniscus' light dispersion. As a result, the photodiode receives less light. This luminance allows for the best response according to this setup configuration and tube dimensions employed in this study. A gray PVC support in Fig. 3 is designed to hold the LEDs and photodiodes in a fixed position. In addition, the gray PVC body acts as an opaque barrier for the light to eliminate interference any between the light produced by the adjacent LEDs.

Instead of using a time-trigger circuit, the output of photodiodes in the new soap flowmeters are digitalized subsequently and sent to a computer for further analysis. Employing computerized data acquisition system allows for greater accuracy. A 20 Hz

analog to digital converter is used in this study; however, a higher speed real time data acquisition system could be utilized for more precise measurements.

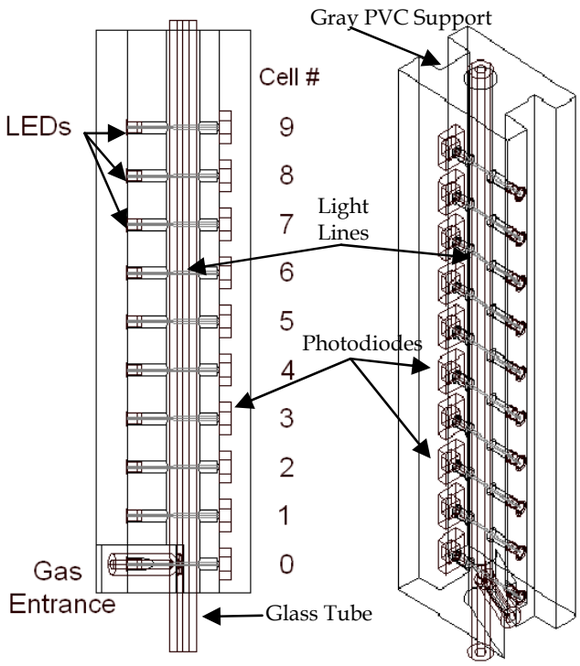

Fig. 3. Position of sensors installed on a 500 µL Supelco flowmeter. Left is the frontal exposure of the isometric view displayed on right. Adapted from Lashkari and Kruczek (2008A)

Accuracy of time measurement without actually increasing the time to be measured or decreasing tube radius is achieved in the new instrument by employing a signal analysis to find the minimum voltage of every pulse. These minima are determined by an interpolation using a 4^{th} order Spline equation fitted to the experimental points. The time interval can then be extracted by comparing the minimum values for two subsequent photodiodes. By increasing the number of experimental points, the accuracy will increase as long as the resolution of an analog to digital converter is high enough. Based on current technology, the time that can be measured by a computer directly is in order of milliseconds; however, real time instruments can provide a much higher accuracy. As a result, having a more advanced real time data acquisition apparatus would provide a more precise measurement of measurement of time intervals, allowing for an increased accuracy of flow measurement.

The developed soap flowmeters were used for the measurement of gas permeation rates of N_2 through a poly(phenylene oxide), PPO, membrane. The permeations were controlled by adjusting the feed pressure of the membrane. The modified soap flowmeter, based on the 500 µL Supelco flowmeter, was capable of automatic measurements of microflows as low as 0.005 cm^3/min. These microflows correspond to the minimum value that can be measured using the smallest commercially available soap flowmeter. The latter, however, utilizes the capillary tube, which has the nominal size of just 50 µL. In comparison to the commercial fully automated SF-1/2 soap flowmeter available from STEC, the minimum flow rate of the new instrument is decreased by nearly two orders of magnitude.

3.1.3 Droplet tracking technique

The principle of the DT technique is the same as that of the soap flowmeter, except that the flow rates are determined by monitoring the movement of a liquid droplet rather than a soap bubble. The orientation of the calibrated tube in the DT method must be horizontal rather than vertical because that of a liquid droplet is much greater than the weight of a liquid bubble. Consequently, gravitational forces that would act on the liquid droplet in the vertical tube would not be negligible, and the pressure gradient across the liquid droplet would not be constant. As a result, the velocity of the liquid droplet in a vertical tube at a steady state would not be constant.

The DT technique is commonly used for measurement of microflows emerging from microchannels (Harley et al., 1995; Zohar et al., 2002; Maurer et al 2003; Colin et al., 2004; Ewart et al., 2006; Pitakarnnop et al, 2010). When the downstream of a capillary is open to atmosphere, the flow measurement can be performed using a soap flowmeter (Celata et al., 2007). However, at these conditions, some research groups, carry out their measurements using the DT technique. This technique cannot be replaced by soap flowmeter measurements when the downstream of the capillary is connected to a constant volume at sub-atmospheric pressures. Studies involving flows in transition and near free molecular regimes require very low downstream pressures. For example, Pitakarnnop et al. (2010) and Ewart et al. (2006) reported flow measurements at downstream pressures of as low as 1,928 Pa and 1,101 Pa, respectively. At such low pressures, a soap bubble and even a soap liquid droplet would quickly evaporate making measurement impossible. For this reason, the liquid used in the DT method must have a very low vapour pressure; typically an oil droplet is used. In their studies, Ewart et al. (2006) used, for example, oil with a vapour pressure of 1.33×10^{-3} Pa.

The liquid droplet is introduced into the capillary typically using a syringe, after which the droplet is allowed to reach constant moving velocity before measurements are taken. The position of the bubble moving in the calibrated part of the capillary is observed visually (Zohar et al., 2002), or with a help of auxiliary instrumentation. The latter includes, the use of opto-electronic sensors (Colin et al., 2004; Pitakarnnop et al., 2010) similar to those used in automated soap flowmeters, or a low power microscope (Harley et al., 1995), or using a high resolution digital camera (Ewart et al., 2006). After measurement, the liquid droplet must be retracted and/or withdrawn from the capillary in order to prepare the system for the next measurement.

Flow rates measured by the DT technique are typically provided in kg/s. Thus, the comparison of minimum flow rates that can be measured with the DT technique and soap flowmeters is not immediately obvious because of different measurement units. Moreover, some research groups provide very low mass flow rates for an individual microchannel by using hundreds of identical microchannels in parallel in a single test section (Shih et al., 1996). As a rule of thumb, the lowest value of the mass flow rate that can be measured by the DT technique in a system with a single microchannel is of the order 10^{-10} kg/s (Morini et al., 2011). However, values much lower than 10^{-10} kg/s have been reported in the literature. For example, Ewart et al. (2006) reported measuring the mass flow of nitrogen as low as 2.68×10^{-12} kg/s. In this case, the measurement was carried out at the pressure of just 1.1 kPa and 296.3 K. Converting this mass flow rate into volumetric flow rate at 1.1 kPa and 296.3 K

leads to approximately 0.013 cm^3/min, which is actually greater than 0.005 cm^3/min that can be measured using the SEG soap flowmeter, having the nominal tube size of 50 μL.

In general, the DT technique is associated with greater uncertainty compared to measurements taken using soap flowmeters. Moreover, its implementation is associated with various problems, some of which include (Ewart et al., 2006):

- Difficulty to introduce the drop oil in the calibrated tube without causing a pressure distortion;
- Formation of several drops rather than a single drop in the calibrated tube, which perturbs the pressure in the tube;
- "Explosion" of a droplet causing a pressure jump in the tube;
- Difficulty in precise estimation of the drop/gas interface position and hence difficulty in following the same point of the interface during the experiment.

The first three problems lead to difficulty in maintaining a constant moving speed of the droplet at steady state conditions, which in combination with the fourth problem may result in significant errors in the measured velocity of the liquid droplet. In addition, another problem occurs in the accurate measurement of the inner diameter of the tube (d_t), which weights the most in determining the mass flow rate (Morini et al., 2011). While this problem is also also applicable to measurements with soap flowmeters, it is probably more eminent in case of the DP technique, which utilizes "homemade" rather than commercial calibrated tubes.

3.1.4 Effect of back diffusion on characterization of semi-permeable materials

The influence of back diffusion of air on flow measurements with soap flowmeters has been recognized by Czubryt and Gesser (1968), and more recently by Guo and Heslop (2004). Because of the influence of back diffusion of air, flow measurements should not be taken in the end section of soap flowmeters, in particular when very small flow rates of gases are involved. If the back diffusing air, or more generally any gas, can reach the flow source and then be transported across the flow source, (which is the case when the flow source is a membrane), the effect of back diffusion may lead to a systematic error in gas permeability coefficients determined when using a soap flowmeter. The following discussion is based on the recently published paper by the current authors (Lashkari and Kruczek, 2008B).

Fig. 4 presents a schematic diagram of a typical CP system used for measuring the permeation rate of gas A through a membrane. The gas permeation rate is evaluated based on the gas flow rate measured by a soap flowmeter, which is attached to the permeate side of the membrane. The soap bubble is introduced at the entrance of a calibrated column and is picked up by the flowing gas. Because of the negligible weight of the soap bubble, the speed of the bubble through the calibrated column can be correlated to the volumetric flow rate of the permeating gas. In the system depicted in Fig. 4, the membrane is open to atmosphere of gas B, which is typically air. If A and B are different gases, B may diffuse towards the membrane and then permeate through the membrane. Since the direction of the diffusion and permeation of B is opposite to the direction of the permeation and flow of A, the diffusion and permeation of B are referred to as back diffusion and back permeation, respectively.

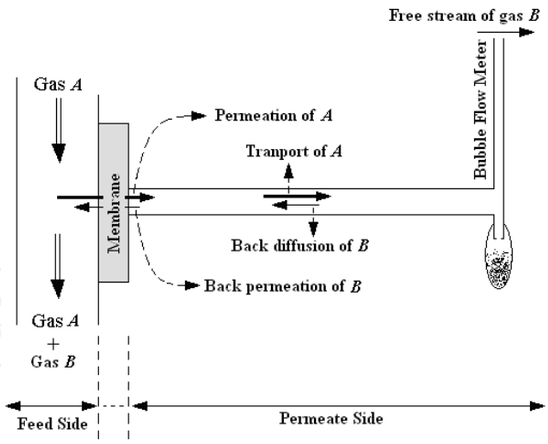

Fig. 4. Measurement of the permeation rate of a gas through a membrane in a constant pressure system. Adapted from Lashkari and Kruczek (2008B).

Treating the membrane in Fig. 4 as a "black box", that is, assuming that the permeability coefficient of A (P_A) is not affected by the presence of B and the permeability coefficient of B (P_B) is not affected by the presence of A in the membrane; the respective fluxes, N_A and N_B, are expressed using Eq. (9):

$$N_A = \frac{P_{m,A}}{L_m}\left(p_{A,f} - p_{A,p}\right) = \frac{P_{m,A}}{L_m}\left(p_f - p_p\left(x_A\right)_P\right) \tag{16}$$

$$N_B = \frac{P_{m,B}}{L_m}\left(p_{B,f} - p_{B,p}\right) = \frac{P_{m,B}}{L_m}\left(0 - p_p\left(1 - \left(x_A\right)_P\right)\right) = -\frac{P_{m,B}}{L_m}p_p\left(1 - \left(x_A\right)_P\right) \tag{17}$$

where: $(x_A)_p$ is the mole fraction of gas A at the permeate side of the membrane. It is important to note that Eq. (16) assumes that the mole fraction of A at the feed side of membrane is equal to unity. This is a reasonable assumption, especially when the feed side is swept with A.

The expression for the permeability coefficient, given by Eq. (10), can be rewritten in a slightly different form, which follows from Eq. (16):

$$P_{m,A} = \frac{L_m N_A}{p_p\left(p_f/p_p - \left(x_A\right)_P\right)} \tag{18}$$

In the case of a single gas permeation test in a CP system, the composition of the permeating gas is not measured, and although not explicitly stated, it is simply assumed that $(x_A)_p$ is equal to unity. Moreover, it is assumed that the experimentally measured gas flux through the membrane (N) corresponds to N_A. With these assumptions, the expression for the permeability coefficient given by Eq. (18) becomes:

$$P_{m,A}\big|_{app} = \frac{L_m N}{p_p\left(p_f/p_p - 1\right)} \tag{19}$$

To distinguish between the permeability coefficients given by Eq. (18) and Eq. (19), the former will be referred to as the actual permeability coefficient and the latter as the apparent permeability coefficient. Given a situation, in which back diffusion and back permeation of B exist, $N \neq N_A$, and $(x_A)_P < 1.0$, consequently $P_{m,A} \neq P_{m,A}\big|_{app}$.

To evaluate the error associated with the apparent permeability coefficient when the phenomena of back diffusion and back permeation are present, it is necessary to realize that for the system depicted in Fig. 4, the experimentally measured gas flux is given by:

$$N = N_A + N_B = Cu \tag{20}$$

where: u is the gas velocity and $C = \sum C_i$ is the total gas concentration. Substitution of Eq. (16) and Eq. (17) into Eq. (20) leads, after rearrangements, to:

$$P_{m,A} = \frac{L_m N}{p_p\left(p_f/p_p - (x_A)_P - \alpha_{BA}\left(1-(x_A)_P\right)\right)} \tag{21}$$

where: $\alpha_{BA} = P_{m,B}/P_{m,A}$. Dividing Eq. (19) by Eq. (21) yields the following expression:

$$\frac{P_{m,A}\big|_{app}}{P_{m,A}} = 1 + (1-\alpha_{BA})\frac{1-(x_A)_P}{p_f/p_p - 1} \tag{22}$$

When $p_f > p_p$, it follows from Eq. (22) that:

$$\text{if} \quad \alpha_{BA} < 1 \quad \Rightarrow \quad P_{m,A}\big|_{app} > P_{m,A}$$

$$\text{if} \quad \alpha_{BA} > 1 \quad \Rightarrow \quad P_{m,A}\big|_{app} < P_{m,A}$$

In the limiting case when $p_f >> p_p$, regardless of α_{BA}, $P_{m,A}\big|_{app} \to P_{m,A}$.

To quantify Eq. (22), it is necessary to evaluate the composition of the gas at the permeate side of the membrane. This requires modelling of back diffusion and the knowledge of the mechanism by which the gas is transported through the membrane. In the following analysis the transport equations describing the phenomenon of back diffusion are developed by assuming that the membrane can be treated as a "black box".

For the purpose of modelling, the CP system presented in Fig. 4 is generalized in Fig. 5. Tube 1 represents a bubble flowmeter. The bubble is made at z_1 and moves towards z_0. Tube 2 is a connecting tube between the membrane cell and the bubble flowmeter. There can be more than two tubes between the membrane and the atmosphere, but for the purpose of modelling the case with two tubes is sufficiently representative. Since there is no velocity field except in longitudinal (z-direction), the continuity equation for a constant density fluid is reduced to:

$$\frac{du}{dz} = 0 \tag{23}$$

where z is distance from the free stream of B (air), i.e. from the outlet of the bubble flowmeter tube.

It is important to emphasize that for typical velocities in gas permeation experiments the pressure drop through the tubes does not affect the velocity field. This can be verified by applying Bernoulli's equation for typical velocities associated with membrane gas permeation. Since the velocity in a tube of constant diameter is constant, the continuity equation yields:

$$u_1\left(\frac{\pi d_1^2}{4}\right)=u_2\left(\frac{\pi d_2^2}{4}\right)=u_m A_m \tag{24}$$

where d is the tube diameter, subscripts 1, 2 and m indicate the tube numbers and the membrane, respectively, and A_m is the membrane area available for gas permeation. The velocity across the membrane can be calculated from:

$$u_m=\frac{\sum_i (N_i)_m}{C} \tag{25}$$

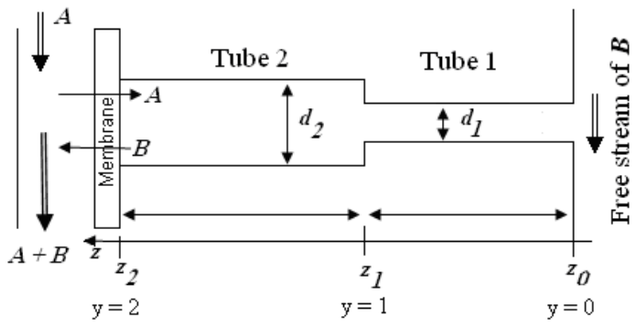

Fig. 5. Schematic representation of a CP system for the purpose of modelling of back diffusion and back permeation. Adapted from Lashkari and Kruczek (2008B).

Combining Eqs. (24) and (25) leads to:

$$u_1=u_m\frac{A_m}{\left(\pi d_1^2/4\right)}=\frac{\sum_i (N_i)_m}{C}\frac{A_m}{\left(\pi d_1^2/4\right)} \tag{26}$$

Assuming that air consists only of N_2 and O_2, gas permeation experiments with single N_2 and O_2 will represent the examples of back diffusion and back permeation in binary systems. In the experiment with O_2, A = O_2 and B = N_2. For the components A and B in a binary system the continuity equations are:

$$\frac{d(N_A)}{dz}=0 \qquad\qquad \frac{d(N_B)}{dz}=0 \tag{27}$$

Applying Fick's first law, the total flux of A in tube k is given by:

$$\left(N_A\right)_k = -CD_{AB}\frac{dx_A}{dz} + x_A\left(Cu_k\right) \tag{28}$$

or

$$\frac{dx_A}{dz} = \frac{u_k}{D_{AB}}\left(x_A - \xi_A\right) \tag{29}$$

where D_{AB} is the diffusivity of A in B, ξ_A is a position independent dimensionless parameter defined by Eq. (30), and subscript k indicates the tube number.

$$\xi_A = \frac{\left(N_A\right)_k}{\left(N_A\right)_k + \left(N_B\right)_k} = \frac{\left(N_A\right)_k}{Cu_k} \tag{30}$$

To obtain the composition profile in the tubes, $x_A(z)$, and thus the gas composition at the permeate side of the membrane, $(x_A)_p$, Eq. (29) must be solved for all tubes. The solution in each tube requires one boundary condition. The composition of the free stream B, which is the composition of air, represents the boundary condition for tube 1. Solving Eq. (29) for tube 1 allows evaluation of the gas composition at z_1, $(x_A)_1$, which represents the boundary condition for tube 2, with which Eq. (29) may be solved in tube 2. Treating the membrane as a black box, ξ_A may be expressed in terms of N_A evaluated from Eqs. (16) and (17) as:

$$\xi_A = \frac{p_f/p_p - \left(x_A\right)_P}{p_f/p_p - \left(x_A\right)_P - \alpha_{BA}\left(1 - \left(x_A\right)_P\right)} \tag{31}$$

Therefore, for a binary system and a two-tube configuration presented in Fig. 5 the following equation becomes applicable:

$$\frac{\xi_A - \left(x_A\right)_P}{\xi_A - \left(x_A\right)_0} = \exp\left(-\frac{u_1}{D_{AB}}\left(l_1 + l_2\left(\frac{d_1}{d_2}\right)^2\right)\right) \tag{32}$$

It is important to note that u_1 in Eq. (32) represents the net velocity of the gas in the bubble flowmeter, a positive number, which can be measured experimentally. In general:

$$\frac{\xi_A - \left(x_A\right)_P}{\xi_A - \left(x_A\right)_0} = \exp\left(-\frac{u_j}{D_{AB}}l_e\right) = \exp\left(-Pe\right) \tag{33}$$

where Pe is the Peclet number ($Pe = u_j l_e / D_{AB}$) in which l_e is an equivalent length of the connecting tubes. For n tubes in series including soap flowmeter as tube j, the general equation for l_e is given by:

$$l_e = \sum_{k=1}^{n} l_k\left(\frac{d_j}{d_k}\right)^2 \tag{34}$$

Eqs. (31) and (33) can be simultaneously solved for the two unknowns $\left(x_A\right)_P$ and ξ_A, and then $P_{m,A}\big|_{app} / P_{m,A}$ can be evaluated using Eq. (22).

The model for back diffusion and back permeation was compared with experimental data generated in single gas permeation experiments with oxygen and nitrogen using a homogeneous PPO membrane, in a CP system equipped with fully automated soap flowmeter capable of measuring the flow rates as low as 0.005 cm^3/min (Lashkari and Kruczek, 2008A). The experimental system also allowed sampling of the permeating gas at three different distances from the membrane in order to compare the experimentally determined gas compositions with the model-predicted values.

The experimental results for the apparent permeability and the composition of the permeating gas as a function of feed pressure confirmed the theoretical trends, but some discrepancies were observed. The discrepancy between the experimental and theoretical results was quantified by a dimensionless correction factor (β), with which Eq.(33) becomes:

$$\frac{\xi_A - (x_A)_P}{\xi_A - (x_A)_0} = \exp(-\beta Pe) \tag{35}$$

The correction factor β, determined by minimizing the least square difference between the theoretical and experimental values using a MATLAB simplex method, was less than unity for all experimental runs. In other words, the experimentally observed effects of back diffusion and back permeation were actually greater than the theoretically predicted effects. In general, the discrepancy based on the composition of permeate was greater than that based on the permeability coefficients; also the discrepancy increased with decrease in the membrane thickness. As the membranes thickness decreases, the flux and thus the net velocity of the gas in tube increases. This indicates that the effects of back diffusion and back permeation might be still present at relatively large *Pe*.

From the point of view of membrane characterization by single gas permeation experiments with N_2 and O_2, the effect of back permeation and back diffusion leads to an underestimation of the permeability coefficient of less permeable gas (N_2) and an overestimation of the permeability coefficient of more permeable gas (O_2). Consequently, the ideal selectivity, α_{O_2/N_2}, will be greatly overestimated. The phenomena of back diffusion and back permeation may explain some "inflated" ideal selectivities reported in the literature.

The obtained experimental results by Lashkari and Kruczek (2008B) suggest running gas permeation tests in a CP system at the conditions for which $Pe \geq 10$. It also appears to be more advantageous to maximize the *Pe* number by increasing the length of the tube connecting the membrane cell with the bubble flow meter rather than by increasing the net velocity of the gas in the soap flow meter column via, for example, an increase in feed pressure and/or by using thinner membranes. However, since maximization of the *Pe* number does not guarantee complete elimination of the effects of back diffusion, it might be advantageous to sample permeating gas or gases near the permeate side of the membrane to allow for the analysis of the permeate composition. Negligible concentrations of back permeating gases in the permeate stream near the membrane would increase reliability of the permeability coefficient determined in a CP system. Even if back permeation effects were not negligible, knowing the exact composition of the permeate stream near the membrane would allow for more accurate calculations of permeability coefficients.

3.2 Constant volume technique

In the constant volume (CV) technique flow measurements are carried out at constant volume and temperature conditions, while changes in pressure are monitored simultaneously. Consequently, Eq. (2) simplifies to:

$$Q = \frac{V}{RT}\frac{dp}{dt} \tag{36}$$

As a rule of thumb, the CV technique allows measurements of much lower flows than the CP technique. Therefore, the CV technique has become a very important tool in characterization of microchannels. In the case of membranes, the CV technique not only allows for the measurement of flows that otherwise could not be measured, but also the determination of the diffusivity coefficient. The resolution of the CV technique and thus the lower limit of flow rates that can be measured depend on the resolution of the pressure sensor. For this reason, it is advantageous to carry out CV flow measurements at very high vacuum. This is not however, always possible, particularly in applications involving microchannel characterizations.

3.2.1 Constant volume technique in membrane characterization

The constant volume (CV) technique has been used for characterization of gas permeation through semi-permeable membranes since the introduction of the latter in the mid nineteenth century (Stannett, 1978). Moreover, since the introduction of a time lag method by Daynes nearly a century ago (Daynes, 1920), which was brought to prominence by Barrer (1939), the CV technique has also been widely used for the evaluation of membrane diffusivity. The CV membrane characterization technique is exclusively employed at the highest vacuum possible.

A common experimental technique in CV systems used to determine the diffusivity involves the procedure, in which the inflow and outflow volumes are evacuated to the lowest possible absolute pressure to degas the membrane or the medium to be tested. The inflow volume is then instantaneously pressurized and the resulting pressure response at the permeate side of the membrane is monitored. If, after pressurization, the concentration of the gas at the feed and the permeate faces of the membrane are constant and the latter remains approximately equal to zero during the entire experiment, the pressure in the receiver as a function of time (t), is determined by (Barrer, 1939):

$$p(t) = \frac{A_m p_f P_m RT}{V v_{STP} L_m}\left[t - \frac{L_m^2}{6D_m} + \frac{2L_m^2}{\pi^2 D_m} \times \sum_{n=1}^{\infty} \frac{(-1)^{n+1}}{n^2} \exp\left(-\frac{D_m n^2 \pi^2 t}{L_m^2} \right) \right] \tag{37}$$

where v_{STP} is the volume of one mole of gas at standard temperature and pressure conditions. It is important to emphasize that p_f in Eq. (37) corresponds to the pressure gradient across the membrane, which implies that the pressure increase at the permeate side of the membrane is negligible compared to p_f. Eq.(37) is graphically presented in Fig. 6. The last term on the right-hand side of Eq. (36) contains an exponential function with a negative argument, which is proportional to t. Consequently, as t increases, this term disappears and the pressure response becomes a linear function of time.

$$p(t) = \frac{A_m p_f P_m RT}{V v_{STP} L_m}\left[t - \frac{L_m^2}{6D_m} \right] \tag{38}$$

The term in front of the bracket in the above equation corresponds to the slope in Fig. 6, which represents dp/dt in Eq. (36). Moreover, this term contains the permeability coefficient, thus P_m can be evaluated from the slope in Fig. 6. The extrapolation of the linear part of the pressure response curve into the time axis represents the time lag (θ_m) of tested membrane. Mathematically, the expression for θ_m is obtained by setting $p(t)$ equal to the initial pressure in the receiver, which is assumed to be zero. Therefore:

$$t = \theta_m = \frac{L_m^2}{6D_m} \tag{39}$$

Consequently, the diffusivity of the membrane can be obtained by rearranging Eq. (39) based on the time lag and the thickness of the membrane. Knowing D_m and P_m, allows for the determination of S_m from Eq. (5). Thus, the time lag method allows for the evaluation of the three gas transport coefficients based on the asymptote of the pressure response curve in a single gas permeation experiment.

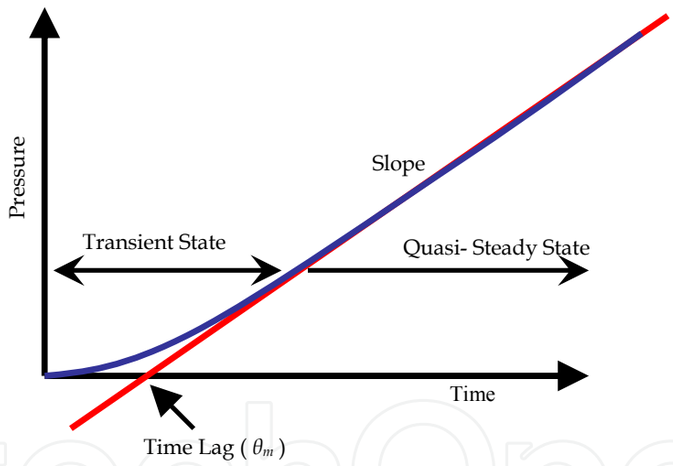

Fig. 6. Expected pressure response of a pressure sensor in a CV system receiver during a time lag experiment.

The heart of the CV system is the receiver, where the gas permeating through the membrane is accumulated and its pressure accurately measured. Early designs of CV systems were based on the Dow gas transmission cell, originally developed in late 1950s (Paul and DiBenedetto, 1965). In that system, the gas accumulates directly under the tested membrane and the volume of the receiver is varied by means of an adapter. It is important to emphasize that the requirement of "constant volume" is not strictly observed in the Dow's cell, because the pressure increase due to gas permeation is measured using a mercury manometer, and as the pressure of the accumulated gas increases, the mercury in the capillary leg is displaced.

Commercial availability of high accuracy, low-range pressure transducers has led to more complex designs of the receiver. Generally, in case of the modern systems, the permeating gas is no longer accumulated directly under the tested membrane, and receiver configurations can be divided into two groups, systems with a single accumulation tank and systems with multiple accumulation tanks (Lashkari and Kruczek, 2010).

An example of a CV system with a single accumulation tank is described by O'Brian et al. (1986). In this system, depending on the anticipated permeation rate, a tank with a correspondingly appropriate volume should be used. However, the range of tank volumes, length and size of tubing used downstream from the membrane are are not commonly provided in the literature. The system described by O'Brian et al. (1986) was modified by Costello and Koros to allow for its use at elevated temperatures; the accumulation tank used in the modified system has volume of 1000 cm^3 (Costello and Koros, 1992). Recently, Al-Juaied and Koros (2006) reported using 1/4 and 1/8 inch tubes and a total receiver volume of 1029 cm^3. Assuming the same size of the accumulation tank in references (Costello and Koros, 1992) and (Al-Juaied and Koros, 2006), 29 cm^3 corresponds to the volume of 1/4 in. and 1/8 in. tubes as well as to the volume associated with valves and fittings downstream from the membrane. CV systems with a single accumulation tank are also used by other research groups (Shishatskii et al., 1996; Bos et al., 1998; Lee et al., 1999).

Unlike in systems with a single accumulation tank, in systems with multiple accumulation tanks can change the receiver volume without exposing the system to atmosphere. The latter is not desirable because re-evacuation of the receiver might be very time consuming. For example, Huvard et al. (1980) reported two weeks as a minimum evacuation time before performing any gas permeation experiments. Stern et al. (1963) provide one of the earliest examples of a system with multiple accumulation tanks, but without any detailed specifications. Based on the schematic diagram provided in this reference, the system consists of three accumulation tanks arranged in parallel. Another example of a three-tank system is described in Kemp (1972), in which two of the tanks are arranged in parallel, while the third tank is in series with the other two. As a result, the volume downstream from the membrane can have five discrete values ranging from 4.77 cm^3 to 108.7 cm^3 (Kemp, 1972). The system reported by Huvard et al. (1980) consists of four accumulation tanks arranged in parallel and 1/4 in. tubes. While the volumes of the accumulation tanks are not reported, according to the schematic diagram, each tank has a different volume. Therefore, the volume of the receiver in that system can have 16 discrete values. Multiple accumulation tanks are also used in the CV system described by Mohammadi et al. (1995), Lin et al. (2000) and Lashkari and Kruczek (2011).

The biggest challenge associated with CV systems operating at a very high vacuum is tightness of the receiver. While operation of the CV systems at high vacuum maximizes the resolution of the measurement, the advantage of high resolution disappears if the tightness of the receiver is compromised. This is because the tightness of the receiver determines the leak rate into the system. Under normal operation protocol, leak rate should be checked before each experiment, and in principle this determined leak rate could be subtracted from the measured flow rate. Nevertheless, when the apparent flow rate is in the order of the leak rate, the reliability of the measurement is compromised. Therefore, whenever possible, it is best to carefully weld tube connections in the receiver, and when welding is not possible

VCR connections with replaceable metal gaskets one should use. The advantages and disadvantages of welding versus VCR, tube fittings are discussed by Moore et al. (2004). All valves in the receiver should be special vacuum valves. The most difficult element to seal in the receiver is the membrane cell. Schumacher and Ferguson (1927) sealed the membrane cell with mercury. Tabe-Mohamadi et al., (1995) used the membrane itself facing two mirror polished plates and reported leak rates below 1.2×10^{-9} cm³/s. On the other hand, Moore et al. (2004) employed a combination of an o-ring with a self-seal membrane masking to seal the membrane cell, and recommended this method for brittle membranes such as carbon molecular sieve membranes.

3.2.2 Constant volume technique in microchannel characterization

The CV technique in microchannel characterization is used only for the measurement of gas flows emerging from microchannels under a specific pressure gradient. CV systems in microchannel characterization are not used while under very high vacuum, but rather over a wide distribution of pressures ranging from near atmospheric to moderate vacuum pressures. In addition, the receivers used in applications involving flow measurements in microchannels are relatively simple, consisting of a tank with a relatively large volume to ensure quasi-steady state conditions during measurement, a sensitive pressure sensor and, a tube connecting the microchannel with the tank and the pressure sensor. On the one hand, the volume of the receiving tank should be large, but on the other hand, if the pressure in the tank is excessively large, the detection of the pressure rise resulting from the microchannel flow becomes difficult, in particular when approaching atmospheric pressure.

Another difficulty with measurements near atmospheric pressure is the influence of small temperature drifts on flow measurement. To understand this problem, Eq. (36) must be presented more generally:

$$Q = \frac{V}{RT}\frac{dp}{dt} - \frac{pV}{RT^2}\frac{dT}{dt} \tag{40}$$

It is evident from Eq.(40) that the effect of temperature variation, dT/dt, on the measured flow is directly proportional to p.

To address the problem of very low resolutions and temperature fluctuations near atmospheric pressures, Arkilic et al. (1997) developed a two-tank CV system. Both tanks in the modified receiver are located downstream of the microchannel. During the test one tank is used to accumulate the gas flowing out of the microchannel, while the other one remains at constant pressure, thus acting as a reference tank. The main advantage of this is solution comes from the fact that instead of measuring the absolute pressure rise, the pressure difference between the two tanks is measured. Consequently, Eq. (39) becomes:

$$Q = \frac{V}{RT}\frac{d(\Delta p)}{dt} - \frac{\Delta pV}{RT^2}\frac{dT}{dt} \tag{41}$$

where Δp is the pressure difference between the reference tank and the working tank. In the case of experiments near atmospheric pressure, Δp at the end of experiments is typically

orders of magnitude less than p. Consequently, the sensitivity of the mass flow rate to the tank temperature fluctuations is reduced by several orders of magnitude, and the minimum flow rate that can be measured in this system is also greatly decreased.

Ewart et al. (2006) developed a system that allows flow measurement by both the DP method and the CV method. While downstream pressure for the two methods are overlapping, the tests involving a relatively high vacuum (absolute pressures less than 1 kPa) were exclusively performed using the CV method. At such low pressures the problems are greatly reduced with regards to the sensitivity of pressure measurement by an absolute pressure transducer, and the effect of temperature fluctuations.

Recently, Pitakarnnop et al. (2010) developed a new setup for gas microflows, in which the CV method is applied at both downstream and upstream of the microchannel, which offers a double check and provides the possibility to compare the measured results for the same flow. The system is also equipped with Peltier modules to maintain a constant temperature. In addition, similarly to the system of Ewart et al. (2006), the system of Pitakarnnop et al. (2010) is also capable of flow measurement by the DT method.

Another challenge to the CV method is to achieve a constant mass flow rate, when applied to measure the flow in microchannels. Unlike the DT method, the receiving volume cannot be excessively large. The same is also true for the inflow volume in the case of the system presented by Pitakarnnop et al. (2010. As the outlet of the microchannel is directly connected to the tank, the outlet pressure keeps changing and is uncontrolled. The inlet pressure must be very carefully adjusted with the passage of time to maintain constant pressure difference between the two tanks. This is very difficult to achieve in practice. Thus, the process of gas flow in the microchannel becomes time-dependent with the CV method (Morini et al., 2011).

3.2.3 Resistance to gas accumulation in high vacuum systems

Although not explicitly stated, measurements in CV systems rely on the assumption that there is no resistance to gas accumulation in the receiver. In other words, as a gas molecule enters the receiver at a specific point, it can be found anywhere within the receiver with the same probability. However, this would require an infinite diffusivity of the molecule in the receiver. In reality, the diffusivity of gas molecules accumulating in receivers that are initially at high vacuum is a finite value. In tubes of small cross-sectional area, which are normally an integral part of modern receivers, the Knudsen number (Kn) is often much greater than unity and the accumulation of the gas occurs at free or near free molecular regime (Kruczek et al., 2005). The diffusivity of molecules accumulating in a circular tube at these conditions can be evaluated from a semi-empirical formula reported by Loab (1961):

$$\mathrm{D} = \frac{\mathrm{pr}^2}{8\mu} + \frac{2}{3}\mathrm{r}\sqrt{\frac{8\mathrm{RT}}{\pi\mathrm{M}}}\left(\frac{1+\mathrm{C_1p}}{1+\mathrm{C_2p}}\right) \tag{42}$$

where p is the mean pressure in the tube, r is the radius of the tube, μ is the dynamic viscosity of the gas, M is the molecular mass of the gas, and C_1 and C_2 are constants, which are determined by solving the following set of equations:

$$\frac{C_1}{C_2} = \frac{3\zeta\sqrt{\frac{\pi M}{RT}}p}{8\sqrt{2}\mu} \tag{43}$$

$$C_2 - C_1 = 0.6117\sqrt{\frac{M}{RT}}\frac{r}{\mu} \tag{44}$$

The coefficient of slip (ζ) is evaluated using Maxwell's deduction from the kinetic theory of gases (Maxwell, 1879):

$$\zeta = \frac{\mu}{p}\sqrt{\frac{\pi RT}{2M}}\left(\frac{2-f}{f}\right) \tag{45}$$

where f is a fraction of gas molecules, which lose the momentum as a result of adsorption and desorption at the walls of tube. While f depends on the nature of the gas and the tube surface, it is usually close to unity (Stacy, 1923). With f=1, solving simultaneously Eqs. (43) and (44) leads to the following expressions for the constants C_1 and C_2:

$$C_1 = 0.8768\sqrt{\frac{M}{RT}}\frac{r}{\mu} \tag{46}$$

$$C_2 = 1.4885\sqrt{\frac{M}{RT}}\frac{r}{\mu} \tag{47}$$

At very low pressures, regardless of the value of f, Eq. (42) approaches the expression for the diffusion coefficient in a free molecular (Knudsen) flow regime:

$$D \to D_K = \frac{2}{3}r\sqrt{\frac{8RT}{\pi M}} \tag{48}$$

For commonly used 1/4 inch stainless steel tubing with r = 0.193 cm and N_2 at 23°C, the free molecular regime (Kn > 10) exists at pressures less than 0.49 Pa. On the other hand, the diffusivity of N_2 does not differ more than 10% from D_K = 0.6 m²/s up to 10 Pa (Kruczek et al., 2006).

Application of the time lag method for the characterization of membranes in CV systems requires the receiver to be initially set at as high a vacuum as possible. The actual initial vacuum in the receiver depends on the quality of a vacuum pump used. Using a rotary pump in series with a turbo molecular pump, Checchetto et al. (2004) reported the initial pressures in the range of low 10^{-6} Pa, while Sanchez et al. (2001) in the range of 10^{-7} Pa. Even without a turbo molecular pump, very low initial pressures are possible. For example Li et al. (2001) reported the initial pressure of 0.1 Pa, while Hirayama et al. (1996) of 0.013 Pa.

From the above considerations it is reasonable to assume that accumulation of gases in tubes of a small cross-sectional area can be described using a constant diffusivity of gas. With this assumption and considering the receiver to be a straight cylinder, the resistance to gas transport downstream from the tested medium may be quantified by the position-dependent time lag, using the following expression (Kruczek et al., 2005):

$$\theta(z) = \frac{l^2}{6D} - \frac{(l-z)^2}{2D} \tag{49}$$

where l is the length of the cylinder, and z is the distance of the pressure sensor from the flow source. Depending on z, i.e., the position where the pressure rise is monitored, $\theta(z)$ may be a positive or a negative number. At the limit of $z = l$, Eq. (49) simplifies to $\theta(l) = l^2/6D$, which corresponds to the maximum positive value, while at other limit of $z = 0$, Eq. (49) simplifies to $\theta(0) = -l^2/3D$, which corresponds to the maximum negative value.

The difference between $\theta(l)$ and $\theta(0)$ implies the existence of a constant pressure gradient within the receiver during a quasi-steady state accumulation. Since the pressure within the receiver is constant before the gas starts to flow into the receiver, there must be a transient period, during which the pressure gradient develops; consequently, the pressure response is a function of position within the receiver. In such a transient period, using Eq. (36) for the evaluation of the flow into the receiver could lead to a very significant error. Moreover, since the accumulation of gas leads to an increase in pressure, there should likely be a transition from the free molecular regime to near-free molecular regime, in which the diffusion coefficient increases with pressure. Thus, the developed pressure gradient within the receiver should gradually decrease as the pressure increases. Both of these effects are illustrated in Fig. 7a, in which the pressure gradient within the receiver first develops, and after reaching the maximum value approximately 50 s from the initiation of the experiment, gradually decreases with time, i.e., as the pressure in the receiver increases (Kruczek et al., 2006). This implies that after the initial transient period, the flow rate determined using Eq. (35) continues to be associated with a small systematic error, which decreases however, as the pressure in the receiver increases, and was verified experimentally by Chapanian et al. (2008).

In real systems, the outflow receiver is never just a straight cylindrical tube; it consists of a series of interconnected tanks to vary the volume of the receiver in order to accommodate a wide range of flow rates into the receiver. Since the Knudsen diffusion coefficient is proportional to the internal radius, the resistance to gas accumulation in tanks should be practically negligible. However, the presence of a resistance-free tank in the outflow receiver greatly magnifies the resistance effect in the tube. Assuming a constant diffusion coefficient in the tube connecting the flow source to the resistance-free tank, the following equation for the position-dependent time lag can be derived (Kruczek et al., 2006):

$$\theta(x) = \frac{l^2/D(l/6 + V/2A)}{1 + V/A} - \frac{(l-x)^2}{2D} - \frac{V(l-x)}{AD} \tag{50}$$

where V is the volume of the tank, and A is the cross sectional area of the tube. With $V = 0$, Eq. (50) simplifies to Eq. (49). On the other hand, with $V > 0$, because of the third term, time lag tends to be a large negative number, leading to an underestimation of the time lag of the tested medium. The error is magnified as the distance between the pressure sensor and the tank, $l - x$, increases. The radius of the connecting tube has a major effect on the error, since A is proportional to r^2, while D is proportional to r.

Experimental verification of the effect of the resistance-free tank is demonstrated by comparing Figs. 7a and 7b, which present the progress of time lag experiments monitored

simultaneously by two identical pressure transducers located at different distances from the membrane in two different configurations of the receiver. The results presented in Fig. 7a were obtained in the configuration consisting of only 1/4 inch tube, while those in Fig. 7b in the configuration, assembled with a large accumulation tank at the end of the tube (Kruczek et al., 2006).

The location of the tank at the end of the tube represents the worst case scenario for the resistance in the tube. Installing the tank closer to the flow source while keeping the same total length of tube in the receiver decreases the "magnifying effect" of the tank (Lashkari et al., 2006). The mathematical model that allows evaluation of the resistance effects in any configuration of the receiver, including the configurations with multiple tanks, was recently developed and verified experimentally by Lashkari and Kruczek (2010).

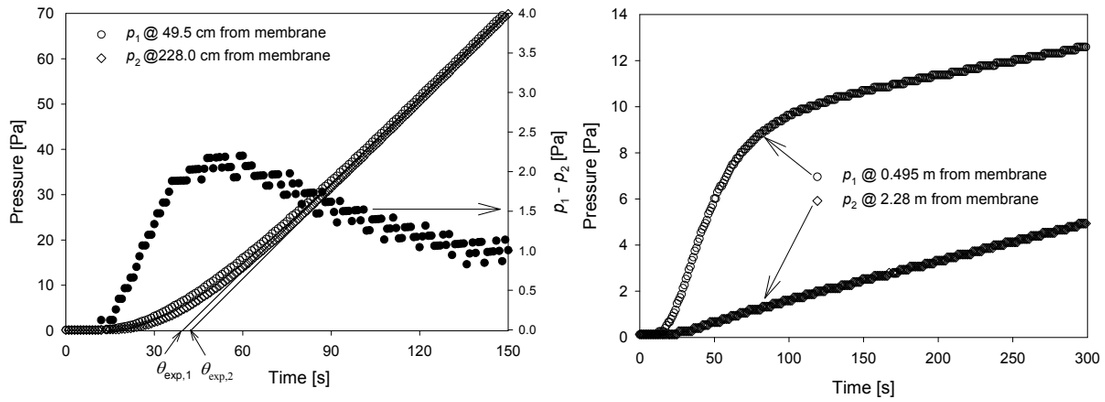

a) b)

Fig. 7. Progress of time lag experiments with a PPO membrane using N_2 at 23°C and at the initial pressure of 0.13 Pa. Experiments monitored simultaneously by two identical pressure transducers installed 0.495 m and 2.28 m from the membrane. Configuration **a):** standard 1/4 inch stainless steel tube of length 2.365 m; feed pressure, p_f = 206.8 kPa. Configuration **b):** standard 1/4" inch steel tube of length 2.415 m with a cylindrical tank of volume $V = 2.250 \times 10^{-3}$ m^3 attached at the end of the tube; feed pressure, p_f = 206.8 kPa. Adapted from Kruczek et al. (2006).

The resistance to gas accumulation in outflow receivers that are initially at high vacuum primarily affects time lag of the medium being tested. In the extreme case of very large resistance shown in Fig. 7b, the resulting apparent time lag based on the pressure transducer located 0.495 m from the membrane is a large negative number implying a negative diffusivity, which obviously does not make physical sense. However, the resistance to gas accumulation may also lead to significant errors in the permeability coefficient. In Fig. 7b, because of a large outflow volume, after 300 s from the initiation of the experiment, the pressure does not exceed 14 Pa, yet the pressure gradient between the positions at 0.495 m and 2.28 m from the membrane is nearly 9 Pa. If the gas were allowed to continue to accumulate in the receiver, this pressure gradient would eventually disappear, but during this time the slope, dp/dt at 0.495 m would be lower than that at 2.28 m Consequently, the measured microflows based on Eq. (35) would depend not only on the location of the pressure transducer, but also on the time frame used for the evaluation of the slope.

The problem of resistance to gas accumulation in CV systems used in microchannel characterization is likely negligible. This is not only because these systems are not operated at very high vacuum, but also because the outflow volume cannot be very large due to the problem with the resolution of the pressure measurements. Conversely, in characterization of microchannels by the DT method, it is desired to have the outflow volume as large as possible to maintain a constant pressure gradient over the microchannel. Therefore, if DT measurements are carried out at downstream pressures of 1 kPa or lower, one should perform calculations suggested by Kruczek et al. (2006) to confirm negligible resistance effects.

3.2.4 Design guidelines for new CV systems

Although CV systems are very commonly used in membrane gas separation labs, to our best knowledge, there are no guidelines for their design. Moreover, as shown in the preceding discussion, the resistance to gas accumulation should be taken into consideration when designing a new CV system. This section summarizes the key points of the design process.

Range of rate of pressure increase

The range of rate of pressure increase, i.e., the range of asymptote slopes (dp/dt), is primarily determined by a pressure transducer. The minimum slope, $dp/dt_{\min}$, depends on the resolution of the selected pressure transducer. Since the resolution is inversely related to the linear range of the transducer, the resolution can in principle be increased by selecting a pressure transducer with a very small linear range. However, apart from the resolution of the pressure sensor, the lowest reliable rate of pressure increase also depends on the tightness of the receiver, which governs the leak rate into the receiver. While the determination of the leak rate is a prerequisite before each experiment in a CV system, and the experimentally determined leak rate can be subtracted from the apparent permeation rate, the actual permeation rate determined this way will be associated with a considerable random error if the leak rate is relatively large.

The maximum slope $dp/dt_{\max}$, which determines the upper measurement range may appear to be primarily determined by the linear range of the selected pressure transducer. When performing a time lag experiment in absence of large resistance to gas accumulation, the pressure response becomes a linear function of time after $3\theta_m$, but to minimize the error in determination of the slope of the asymptote, the time lag experiment should be carried out for at least the period corresponding to 4 θ_m, and the permeate pressure after the time corresponding to 4 θ_m and preferably 10 θ_m should be below the upper limit for the linear range of the pressure transducer. On the other hand, considering possible effects of increasing permeate pressure (Lashkari, 2008), it might be advantageous to keep the permeate pressure well below the upper limit for the linear range of the pressure transducer. In addition, if accumulation in the receiver is influenced by the resistance effects, keeping the permeate pressure below 10-20 Pa would minimize the variation of the diffusion coefficient downstream from the membrane, which would allow a better recovery of membrane properties (Lashkari and Kruczek, 2012). Consequently, the upper measurement range might be an order of magnitude lower then that arising from the upper limit of the linear range of the utilized pressure transducer.

Minimum volume of the receiver and minimum permeation rate

The minimum volume of the receiver (V_{min}) along with dp/dt_{min} is the critical design parameter when the system is to be used for the evaluation of transport properties of barrier materials, because barrier materials are associated with very low permeability coefficients and thus very low gas permeation rates (Q). The latter should still be significantly greater than the maximum leak rate into the receiver. Consequently, it is possible to set a reasonable limit on the minimum permeation rate (Q_{min}). Knowing Q_{min}, the minimum volume of the receiver can be evaluated by rearranging the ideal gas law:

$$V_{min} = \left(\frac{RT}{v_{STP}} \right) \frac{Q_{min}}{Z_{min}} \tag{51}$$

It should be noted that while the absolute temperature (T) is also directly proportional to V_{min}, gas permeation experiments are typically performed at ambient or slightly above ambient (35^{o}C) temperatures.

In practice, V_{min} is typically determined by the volume of tubing when all tanks are excluded from the outflow volume. In turn, the volume of tubing depends on their length and cross-sectional area. It is important to emphasize that actual V_{min} is always greater than the volume of tubing because of the presence of dead volumes associated with membrane cells, pressure transducer(s), valves and other fittings. According to Lashkari and Kruczek (2010), the length of tubing should be minimized for the physical dimensions of the accumulation tanks and the pressure transducer, while their diameters should be maximized. In practice, tubing with the diameters of at least 1/2 inch are recommended. On the other hand, without knowing the number and the size of the accumulation tanks it is not possible to estimate the required length of tubes and thus the resulting volume of the system when all tanks are excluded. Therefore, it might be advantageous to have the ability to isolate a section of tubing downstream from the membrane cell with the volume corresponding to V_{min} determined from Eq. (51) rather, than letting this parameter be determined by the total length of tubing. The section of tubing that determines V_{min} should of course be equipped with its own pressure transducer. The location of the pressure sensor upstream from accumulation tank(s) is the worst one considering the resistance to gas accumulation, because is it associated with a relatively large negative time lag (Lashkari and Kruczek, 2010). Consequently, it might be necessary to have two pressure sensors in the receiver, one upstream from the accumulation tank(s) for the measurements involving V_{min} and another one downstream from the accumulation tanks for all other measurements.

Maximum volume and maximum permeation rate

In principle, there is no upper limit on permeation rate that could be evaluated in a CV system, because even for very high Q one can find V for which the restrictions on dp/dt_{max} discussed previously will be observed. However, from the practical point of view there are two important considerations that may allow setting the maximum permeation rate (Q_{max}) and the maximum volume of the receiver (V_{max}).

The major advantage of CV systems compared to constant pressure (CP) systems is the ability of continuously monitor of very low permeation rates. However, when the expected permeation rates are greater than 0.1 cm^3/min and definitely when they are greater than 0.5

cm^3/min, it might be more advantageous to evaluate the diffusion, permeability, and solubility coefficients in a constant pressure system using the theoretical framework presented by Ziegel (1969), rather than using a CV system.

Setting the Q_{max} along with previously established Z_{max} will allow determination of V_{max}. Limiting Q_{max} and thus V_{max} is also advantageous from the perspective of minimization of the resistance to gas accumulation. Although without knowing the exact configuration of the receiver and the location of the pressure sensor it is not possible to evaluate the resistance effects, knowing V_{max}, and the length and the diameter of tubing corresponding to V_{min} one can evaluate the position-dependent time lag along the tube using Eq. (49), which is a special case of the general equation derived by Lashkari and Kruczek (2010). To minimize the resistance to gas accumulation it is better to split the volume into more than one accumulation tank. On the other hand, such a split increases the required length of tubing, which in turn, increases the resistance. Consequently, evaluation of the resistance effects for V_{max} attached to the end of tube of length l_{min} will provide some rough resistance values, which could be expected in the final design.

The minimum number of accumulation tanks and their arrangement

To determine the number of accumulation tanks we start from rearranging Eq. (51) to determine the maximum flow rate ($Q_{max,1}$) that can be measured in the previously determined V_{min}:

$$Q_{max,1} = V_{min} Z_{max} \left(\frac{v_{STP}}{RT} \right) \tag{52}$$

If $Q_{max,1} < Q_{max}$, it is necessary to increase the volume of the receiver by ΔV_1. Setting $Q_{max,1}$ to be the minimum permeation rate to be measured in the increased volume of the receiver, the required volume increment can be evaluated from the following equation:

$$V_{min} + \Delta V_1 = \left(\frac{RT}{v_{STP}} \right) \frac{Q_{max,1}}{Z_{min}} \tag{53}$$

The maximum flow rate in the increased volume ($Q_{max,2}$) is determined from Eq.(53) in which V_{min} is replaced by $V_{min} + \Delta V_1$ and the process continues until $Q_{max,n} \geq Q_{max}$. At this point: $V_{min} + \sum_{1}^{n} \Delta V_i \geq V_{max}$. Consequently, following this simple procedure allows evaluation of the number of the required volume increases (n) in the receiver between the predetermined V_{min} and V_{max}, as well as, the value of each increment (ΔV_i). The number of required volume increases corresponds to the minimum number of accumulation tanks in the receiver, while ΔV_is correspond the volumes of the respective tanks.

Since the accumulation tanks are available in a discrete rather than a continuous size range, incremental volume increases between V_{min} and V_{max} according to the above procedure may not be possible. In this case, one should select accumulation tanks with volumes closest but smaller than the respective volumes corresponding to the minimum number of accumulation tanks. This will likely increase the number of the required accumulation tanks and will lead to some measurement overlaps, but at the same time, it will ensure covering the entire range of permeation rates.

It is also important to emphasize that volume increase resulting from adding an accumulation tank is always greater than the actual volume of the added tank because of the necessary extra length of tubing. The volume increment associated with extra tubing should be taken into consideration, in particular when 1/2 inch or larger tubes are utilized.

The tanks can be arranged in parallel or in series. In the case of a series arrangement, the extra volume of tubing associated with each increment can be accurately evaluated. On the other hand, within a parallel configuration, the extra volume of tubing is the same regardless of the number of accumulation tanks utilized in particular configuration (Lashkari and Kruczek, 2010). Moreover, this extra volume of tubing is not known until the number of the required accumulation tanks is established. On the other hand, parallel configuration has one practical advantage over series configuration; the rate of pressure increase in any configuration of the receiver can be monitored using a single pressure transducer installed on the main line regardless of the number of accumulation tanks. In the case of a series configuration, each accumulation tank must be equipped with its own pressure transducer. Therefore, the parallel configuration of accumulation tanks is normally used in multi-tank CV systems. If parallel configuration is selected, and the number and the volumes of the accumulation tanks are established, it is important to verify that covering the entire range of flow measurement, in particular the flow range associated with the first volume increment. This is because of extra length of tubing associated with accumulation tanks. If there are any discontinuities within the flow range, it might be necessary to select smaller tank(s).

After the above design process is completed and subsequently the configuration of the receiver is established, it is now possible to evaluate the anticipated resistance effect using the analytical equations developed by Lashkari and Kruczek (2010). Consequently, it is possible to generate a figure, which maps the position-dependent time lag within the receiver in different possible configurations. If the above guidelines are followed, in particular the 1/2 inch tubes are used and reasonable limits on $Q_{\max}$ and hence $V_{\max}$ are set, the magnitude of the position-dependent time lag should be comparable or even smaller than for the system presented by Lashkari and Kruczek (2012).

Inflow part of CV system

One of the assumptions of the time lag method is that the feed pressure can be increased in a step-wise manner. Favre et al. (2002) investigated the effect of imperfect feed pressure rise on membrane response. They approximated the feed pressure rise by a first order kinetics and concluded that any time delay in the pressure rise would be added to the membrane's time lag. There are couple of simple remedies to reduce the effects of imperfect pressure rise including a time delay in reaching the set value, an overshoot, and a time-dependent pressure decrease. First of all, a relatively large buffer tank should be installed upstream from the membrane. The volume of the buffer tank should be such that when the pressure in the receiver operating in the configuration corresponding to $V_{\max}$ increases to its maximum allowed value, the change in the buffer tank pressure should be negligible. Creating a step change in feed pressure using a gas regulator connected to a pressurized cylinder without a buffer tank creates a problem, because gas regulators have internal dynamics, and are activated with a sudden change in the cylinder pressure during initiation of a time lag experiment. The gas regulator should only be used to fill the buffer

tank and then should be disconnected from the inflow volume by means of a regular valve. The buffer tank should also be isolated from the membrane cell by a special vacuum valve. Once the desired pressure is established in the buffer tank, opening this valve initiates the actual time lag experiment. Consequently, using a vacuum solenoid valve is advantageous because it ensures recording a proper "zero time" and allows a sudden and repeatable opening of this valve, which helps to achieve a perfect step change in feed pressure.

The volume between the solenoid vacuum valve and the membrane should be negligible compared to the volume of the buffer tank. This volume should also be connected to the outflow volume to allow evacuation of both sides of the membrane before an experiment. In addition, O'Brien et al. (1986) recommends having an atmospheric pressure rupture disk on the receiver in case of membrane rupture to protect costly pressure transducers installed in the receiver.

4. Conclusion

The measurements of microflows in characterization of microchannels by the CP, or more specifically by the DP and CV methods are challenging. Since the purpose of the characterization of microchannels is to measure the flow under different pressure gradients, the upstream and downstream ends of the tested microchannel are normally connected to finite volume tanks maintained at different pressures. In case of the DT measurements, the volumes of the tanks can be maximized to maintain a relatively constant pressure gradient. Yet, it is difficult to maintain a constant speed of the droplet in the calibrated tube even at presumably constant pressure gradients. In the case of the CV technique, because of a trade-off between the resolution of the pressure measurement and maintaining a constant pressure gradient across the microchannel, accurate flow measurements are even more challenging.

On the other hand, because of the generally very large resistance to gas transport imposed by a membrane, it is much easier to maintain constant pressure gradients during the characterization of membranes. Moreover, since the CV measurements involving membranes are normally carried out at very high vacuum, the problems associated with the resolution of the pressure measurements and temperature fluctuations do not practically exist. The CP systems used in membrane characterization are open to atmosphere, which allows to carry out the flow measurement at truly constant pressure conditions. Despite these "inherent" advantages, the characterization of membranes using the CP and CV techniques is associated with some unique difficulties, which had been recognized only recently.

The measurements of gas permeation rate in open CP systems may be influenced by the phenomena of back diffusion and back permeation. A simple mathematical model derived from first principles, was presented in this Chapter, allowing for a quick assessment if these phenomena are negligible or not. On the other hand, while the theoretical trends related to back permeation and back diffusion are confirmed experimentally, the magnitude of the systematic error and also the range of conditions at which this systematic error exists are considerably greater than the theoretical predictions.

In the case of measurements involving the CV method, while high vacuum conditions eliminate the problems of pressure resolution and temperature fluctuations, they may lead to gas accumulation resistance. This phenomenon primarily affects the experimentally measured time lag, and thus membrane diffusivity, but it also affects the experimental permeability coefficient. A step-by step procedure for the design of new CV systems is very useful to minimize the resistance effects. However, the complete elimination of the resistance to gas accumulation downstream from the membrane may not be possible, in particular when complex configurations of the receiver are involved. It is therefore of primary importance to understand this phenomenon to be able to correct the existing data and to recover the actual properties of the membrane. A similar approach is also applicable in case of the phenomena of back diffusion and back permeation; they must be well understood in order to be able to interpret the data influenced by these phenomena.

5. Acknowledgment

The authors acknowledge the financial support from NSERC Canada. BK acknowledges the warm hospitality of Mr. and Mrs. Młynarczyk during his stay in Poland, where most of this Chapter was written.

6. References

Al-Juaied, M.; Koros, W.J. (2006). Performance of Natural Gas Membranes in the Presence of Heavy Hydrocarbons, *J. Membr. Sci*., Vol.174, pp. 227-243.

Arenas, A.; Victoria, L.; Ibaňez, J.A. (1995). A Time-Integration-Based Measurement Circuit for a Soap Bubble Flow-Meter Using Optical Fibre Sensors. *Mass. Sci. Technol*. Vol.6, pp. 435-436.

Arkilic, E.B.; Schmidth, M.A & Breuer, K.S. (1998). Sub-Nanomol per Second Flow Measurement Near Atmospheric Pressure. *Experiments in Fluids,* Vol.25, pp. 37-41.

Bailey, B.J.; Ferguson, J.A.; Moses, J.L. (1968). Two Flowmeters Using Electronic Timing *J. Sci. Instrum*. (*J. Phys. E*), Series 2 Vol.1, pp. 562-563.

Barigou, M.; Davidson, J.F. (1993). The Fluid Mechanics of the Soap Film Meter. *Chem. Eng. Sci*., Vol.48(14), pp. 2587-2597.

Barigou, M.; Deshpande, N.S.; Wiggers, F.N. (2003). Numerical Simulation of the Steady Movement of a Foam Film in a Tube. *Trans. Ind. Chem. Eng*, Vol 81, Part A (July 2003) 623-630

Barr, G. (1934). Two Designs of Flow-Meter, and a Method of Calibration. *J. Sci. Instrum*. V.11, pp. 321-324.

Barrer, R.M. (1939). Permeation, Diffusion and Solution of Gases in Organic Polymers. *Trans. Farad. Soc*., Vol.35, pp. 628-643.

Bos, A.; Pünt, I.G.M.; Wessling, M.; Strthmann, H. (1998). Plasticization-Resistanct Glassy Polyimide Membranes for CO_2/CH_4 Separations. *Sep. Pur. Tech*., Vol.14, pp. 27-39.

Celata, G.P.; Cumo, M.; McPhail, S.J.; Tesfagabir, L.; Zummo, G. (2007). Experimental Study on Compressible Flow in Microtubes. *Int. J. Heat Fluid. Flow*. Vol.28, pp. 28-36.

Chapanian, R.; Shemshaki, F.; Kruczek, B. (2008). Error in Measurement of Gas Flow Rate by the Pressure Rise Technique Arising from the Resistance to Accumulation of Gases in Vacuum Tubes. *Can. J. Chem. Eng*., Vol.86(4), pp. 712-719.

Checchetto, R.; Bazzanella, N.; Patton, B.; Miotello, A. (2004). Palladium Membranes Prepared by R. F. Magnetron Sputtering for Hydrogen Surification. *Surface and Coatings Tech*., Vol.177-178, p. 73.

Colin, S.; Lalonde, P.; Caen, R. (2004). Validation of a Second-Order Slip Flow Model in Rectangular Microchannels. *Heat Transf. Eng*., Vol.25(3), pp. 25-30.

Concus, P. (1968). Static Menisci in a Vertical Right Circular Cylinder, *J. Fluid Mech*., Vol.34(3), pp. 481-495.

Costello, L.M.; Koros, W.J. (1992). Temperature Dependence of Gas Sorption and Transport Properties in Polymers: Measurement and Applications. *Ind. Eng. Chem. Res*., Vol.31, pp. 2708-2714.

Czubryt, J.J.; H.D. Gesser, H.D. (1968). Part I - Inaccuracy of the Moving Bubble Flowmeter in the Low Flow Rate Region, *J. Gas Chromat*. Vol.6, pp. 528-530.

Daynes, H.A. (1920). The process of diffusion through a rubber membrane. *Roy. Soc. Proc*., Vol.97, pp. 286-307.

Deissler, R.G. (1964). An Analysis of Second Order Slip Flow and Temperature-Jump Boundary Conditions for Rarefied Gases. *Int. J. Heat Mass Transf*., Vol.7, pp. 681-694.

Ewart, T.; Perrier, P.; Graur, I.A.; Meolans, J.G. (2006). Mass Flow Rate Measurements in Gas Micro Flows. *Experiments in Fluids.* Vol.41, pp. 487-498.

Ewart, T.; Perrier, P.; Graur, I.A.; Meolans, J.G. (2007). Mass Flow Rate Measurements in a Microchannel, From Hydrodynamic to Near Free Molecular Regimes. *J. Fluid. Mech.,* Vol.584, pp. 337-356.

Exner, F. (1875). Über den Durchgang der Gase durch Flüssigkeitslamellen. *Pogg. Ann. Phys. Chem*., V.231, p.321.

Favre, E.; Morliere, N.; Roizard, D. (2002). Experimental Evidence and Implications of an Imperfect Upstream Pressure Step for the Time-Lag Technique. *J. Membr. Sci*., Vol.207, pp. 59–72.

Guo, J.; Heslop, M.J. (2004). Diffusion Problems of Soap-Film Flowmeter When Measuring Very Low-Rate Gas Flow. *Flow Meas. Instrum.* Vol.15, pp. 331-334.

Hadjiconstantinou, N.G. (2003). Comment on Cercignani's Second Order Slip Coefficient. *Phys. Fluids,* Vol.15(8), pp. 2352-2354.

Harley, J.; Huang, Y.; Bau, H.; Zemel, J. (1995). Gas Flow in Microchannels. *J. Fluid. Mech.*, Vol.284, pp. 257-274.

Heslop, M.J.; Mason, G.; Provatas, A. (1995). Comments on the Pressure Produced by a Soap Film Meter. *Chem. Eng. Sci*., Vol.50(15), pp. 2495-2497.

Hirayama, Y; Yoshinaga, T.; Kusuki, Y.; Ninomiya, K.; Sakakibara, T.; Tamari, T. (1996). Relation of Gas Permeability with Structure of Aromatic Polyimides I. *J. Membr. Sci*., Vol.111, p. 169.

Huvard, G.S.; Stannett, V.S.; Koros, W.J.; Hopfenberg, H.B. (1980). The Pressure Dependence of CO_2 Sorption and Permeation in Poly(Acrylonitrile). *J. Membr. Sci*., Vol.6, pp. 185-201.

Jousten, K.; Menzer, H. (2002). A New Fully Automated Gas Flow Meter at the PTB for Flow Rates Between 10^{-13} mol/s and 10^{-6} mol/s. *Metrologia*, Vol.39(6), pp. 519-529.

Kemp, D.R. (1972). The Diffusion Time Lag in Heterogeneous Polymer Membranes. PhD Dissertation, University of Texas at Austin, USA.

Knudsen, M. (1909). Die Gesetze der Molekularstromung und der Inneren Riebungsstromung der Gaze Durch Rohen. *Annu. Phys. (Leipzig).* Vol.28, p.130.

Kruczek, B.; Frisch, H.L.; Chapanian, R. (2005). Analytical Solution for the Effective Time Lag of a Membrane in a Permeate Tube Collector in which Knudsen Flow Regime Exists. *J. Membr. Sci*., Vol.256, pp. 57-63.

Kruczek, B.; Shemshaki, F.; Lashkari, S.; Chapanian, R.; Frisch, H.L. (2006). Effect of a Resistance-Free Tank on the Resistance to Gas Transport in High Vacuum Tube. *J. Membr. Sci.*, Vol.280, pp. 29-36.

Lashkari, S. (2008). Fundamental Aspects of Membrane Characterization by Constant Volume and Constant Pressure Techniques. PhD Dissertation, University of Ottawa, Canada.

Lashkari, S.; Kruczek, B. (2008A). Development of a Fully Automated Soap Flowmeter for Micro Flow Measurements. *J. Flow Meas. Instrum*. Vol.19(6), pp. 397-403.

Lashkari, S.; Kruczek, B. (2008B). Effect of Back Diffusion and Back Permeation of Air on Membrane Characterization in Constant Pressure System. *J. Membr. Sci*., Vol.324, pp. 162-172.

Lashkari, S.; Kruczek, B. (2010). Effect of Resistance to Gas Accumulation in Multi-Tank Receivers on Membrane Characterization by the Time Lag Method. Analytical Approach for Optimization of the Receiver. *J. Membr. Sci*., Vol.360, pp. 442-453.

Lashkari, S.; Kruczek, B. (2012). Reconciliation of Membrane Properties from the Data Influenced by Resistance to Accumulation of Gases in Constant Volume Systems. Desalination, Vol.287 pp. 178-182.

Lashkari, S.; Kruczek, B.; Frisch, H.L. (2006). General Solution for the Time Lag of a Single-Tank Receiver in the Knudsen Flow Regime and its Implications for the Receiver's Configuration. *J. Membr. Sci*., Vol.283, p. 88-101.

Lee, Y.M.; Ha, S.Y.; Lee, Y.K.; Suh, D.H.; Hong, S.Y. (1999). Gas Separation Through Conductive Polymer Membrane. 2. Polyaniline Membranes with O_2 Selectivity. *Ind. Eng. Chem. Res*., Vol.38, pp. 1917.

Levy, A. (1964). The Accuracy of the Bubble Meter Method for Gas Flow Measurements. *J. Sci. Instrum*., Vol.41, pp. 449-453.

Li, X-G.; Kresse, I.; Springer, J.; Nissen, J.; Yang, Y.-L. (2001). Morphology and Gas Permselectivity of Blend Membrane of Polyvinylpyridine with Ethylcellulose. *Polymer*, Vol.42, p. 6859.

Lin, W.-H.; Vora, R.H.; Chung, T.-S. (2000). Gas Transport Properties of 6FDA-Durene/1,4-Phenylenediamine (pPDA) Copolyimides. *J. Polym. Sci., Part B: Polym. Phys*., Vol.38, pp. 2703.

Loeb, L.B. (1961). The Kinetic Theory of Gases. pp. 278-300. Dover Publications, Inc. New York, USA.

Maurer, J.; Tabeling, P.; Joseph. P.; Willaime, H. (2003). Second-Order Slip Laws in Microchannels for Helium and Nitrogen. *Phys. Fluids.* Vol.15, No.9, pp. 2613-2621.

Maxwell, J. (1879) On stress in rarefied gases arising from inequalities of temperature. *Philos. Trans. R. Soc. London,* Vol.170, pp. 170-231.

McCulloh, K. E.;. Tilford, C.R; Ehrlich, C.D.; Long, F.G. (1987). Low-Range Flowmeters for Use with Vacuum and Leak Standards. *J. Vac. Sci. Technol. A*, Vol.5, pp. 376-381.

Moore, T.T.; Damle, S.; Williams, P.J.; Koros, W.J. (2004). Characterization of Low Permeability Gas Separation and Barrier Materials; Design and Operation Considerations. *J. Membr. Sci*., Vol.245(1-2), pp. 227-231.

Morini, G.L.; Yang, Y.; Chalabi, H.; Lorenzi, M. (2011). A Critical Review of the Measurement Techniques for the Analysis of Gas Microflows Through Microchannels. *Exp. Therm. Fluid Sci.* Vol.35, pp. 849-865.

O'Brien, K.C.; Koros, W.J.; Barbari, T.A.; Sanders, E.S. (1986). A New Technique for the Measurement of Multicomponent Gas Transport Through Polymeric Films. *J. Membr. Sci*., Vol.29, pp. 229-238.

Paul, D.R.; DiBenedetto, T. (1965). Diffusion in Amourphous Polymers. *J. Polym. Sci. Part C*, Vol.10, pp. 17-44.

Pitakarnnop, J.; Varoutis, S.; Valougeorgis, S.G.; Baldas, L.; Colin, S. (2010). A Novel Experimental Setup for Gas Microflows. *Microfluid Nanofluid*. Vol.8, pp. 57-72.

Sanchez, J.; Gijiu, C.L.; Hynek, V.; Muntean, O.; Julbe, A. (2001). The Application of Transient Time-Lag Method for the Diffusion Coefficient Estimation on Zeolites Composite Membranes. *Sep. Pur. Tech*., Vol. 25, p. 467.

Schumacher, E.E.; Ferguson, L. (1927). A Convenient Apparatus for Measuring the Diffusion of Gases and Vapours Through Membranes. *J. Am. Chem. Soc*. Vol.49, pp. 427-28.

Shih, J.C.; Ho, C.; Liu, J.; Tai, Y. (1996). Monatomic and Polyatomic Gas Flow Through Uniform Microchannels. *ASME DSC.* Vol.(59), pp. 197-203.

Shishatskii, A.M.; Yampol'skii, Yu.P.; Peinemann, K.-V. (1996). Effects of Film Thickness and Density on Gas Permeation Parameters of Glassy Polymers. *J. Membr. Sci*., Vol.112, pp. 275-285.

Stacy, L.J. (1923). A Determination by the Constant Deflection Method of the Value of the Coefficient of Slip for Rough and for Smooth Surfaces in Air. *Phys. Rev*., Vol.21, p. 239.

Stannett, V.T. (1978). The Transport of Gases in Synthetic Polymeric Membranes — A Historic Perspective. *J. Membr. Sci*., Vol.3(2), pp. 97-115.

Stern, S.A.; Gareis, P.J.; Sinclair, T.F.; Mohr, P.H. (1963). Performance of a Versatile Variable-Volume Permeability Cell. Comparison of Gas Permeability Measurements by the Variable-Volume and Variable-Pressure Methods. *J. Appl. Polym. Sci*., Vol.7, 2035-2051.

Tabe Mohammadi, A.; Matsuura, T.; Sourirajan, S. (1995). Design and Construction of Gas Permeation System for the Measurement of Low Permeation Rates and Permeate Compositions. *J. Membr. Sci*., Vol.98, pp. 281-286.

Zohar, Y.; Lee, S.Y.K.; Li, W.Y.; Jiang, L.; Tong, P. (2002). Subsonic Gas Flow in Straight and Uniform Microchannel. *J. Fluid Mech.* Vol.472, pp. 125-151.

Zolandz, R.; Fleming, G.K. (1992). Gas Permeation, In: *Membrane Handbook* H. Sirkar (Ed.), , Van Nostrand Reinhold, New York, USA.

Ziegel, K.D.; Frensdorff, H.K.; Blair, D.E. (1969). Measurement of Hydrogen Transport in Poly-(Vinyl Fluoride) Films by the Permeation-Rate Method. *J. Polym. Sci.: Part A.*, Vol.2(7), pp. 809-819.

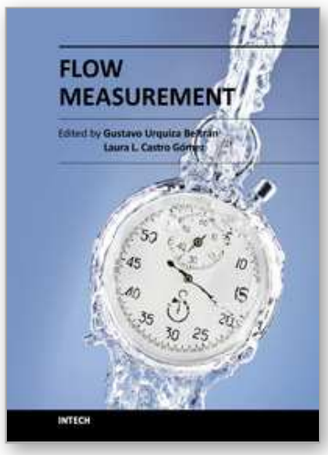

Flow Measurement

Edited by Dr. Gustavo Urquiza

ISBN 978-953-51-0390-5
Hard cover, 184 pages
Publisher InTech
Published online 28, March, 2012
Published in print edition March, 2012

The Flow Measurement book comprises different topics. The book is divided in four sections. The first section deals with the basic theories and application in microflows, including all the difficulties that such phenomenon implies. The second section includes topics related to the measurement of biphasic flows, such as separation of different phases to perform its individual measurement and other experimental methods. The third section deals with the development of various experiments and devices for gas flow, principally air and combustible gases. The last section presents 2 chapters on the theory and methods to perform flow measurements indirectly by means on pressure changes, applied on large and small flows.

How to reference

In order to correctly reference this scholarly work, feel free to copy and paste the following:

Boguslaw Kruczek and Siamak Lashkari (2012). Challenges in Microflow Measurements, Flow Measurement, Dr. Gustavo Urquiza (Ed.), ISBN: 978-953-51-0390-5, InTech, Available from: http://www.intechopen.com/books/flow-measurement/challenges-in-microflow-measurements

INTECH
open science | open minds

InTech Europe
University Campus STeP Ri
Slavka Krautzeka 83/A
51000 Rijeka, Croatia
Phone: +385 (51) 770 447
Fax: +385 (51) 686 166
www.intechopen.com

InTech China
Unit 405, Office Block, Hotel Equatorial Shanghai
No.65, Yan An Road (West), Shanghai, 200040, China
中国上海市延安西路65号上海国际贵都大饭店办公楼405单元
Phone: +86-21-62489820
Fax: +86-21-62489821

IntechOpen